Analysis of the formation of a vinyltrimethoxysilane film on 1010 carbon steel using electrochemical techniques

Bruno Souza Fernandes
Department of Chemical Engineering, Federal University of Bahia, Salvador, Brazil

Kleber Gustavo da Silva Souza
Science and Technology Department, State University of Santa Cruz, Ilhéus, Brazil

Idalina Vieira Aoki
Department of Chemical Engineering, University of São Paulo, São Paulo, Brazil, and

Franco Dani Rico Amado
Science and Technology Department, State University of Santa Cruz, Ilhéus, Brazil

Abstract

Purpose – The application of coatings on metal substrates can provide an increase in corrosion resistance in the environment where the material is employed. The use of silane causes low environmental impact and may represent an alternative to replace chromates and phosphates applied as a pretreatment prior to surface painting. The objective of this study was to evaluate experimental parameters for the investigation of the formation of a vinyltrimethoxysilane (VTMOS) monolayer on 1010 carbon steel applying electrochemical techniques.

Design/methodology/approach – A total of 24 types of coated samples were obtained, following three 2^3 factorial design of experiments (DOE), and one uncoated. The VTMOS monolayer was formed by hand dip process, followed by curing in a stove, using substrates of sanded, pickled and degreased 1010 carbon steel and hydrolyzed silane.

Findings – The results of coated samples were satisfactory as compared to those of uncoated carbon steel, as the former were better protected against corrosion.

Originality/value – This paper shows an evaluation of experimental parameters that influence the formation of a film of silane VTMOS on 1010 carbon steel by means of electrochemical techniques. The results indicated that the silane monolayer VTMOS promotes enhanced properties that prevent corrosion of 1010 carbon steel and the method of film formation directly influences the properties of such protection.

Keywords Carbon steel, Vinyltrimethoxysilane, Silane, Corrosion, Electrochemical techniques, Steel, Corrosion resistance

Paper type Research paper

1. Introduction

Phosphating and chromating pretreatments are applied to steels before they pass through the painting process used in industry as methods to improve corrosion prevention and enhance coating adhesion characteristics. These processes are still widely used because of their efficiency. However, due to high operational costs, coupled with environmental issues and the costs associated with the treatment of the residues produced that are toxic and carcinogenic, efficient "green" pretreatments are being sought to replace them. One of the potential alternatives involves the use of silanes (functional or organofunctional), which generate residues of low toxicity, requiring minimal treatment for appropriate discharge, and which offer protection against corrosion and adhesion (Ran *et al.*, 2011; Metroke *et al.*, 2009; Palanivel *et al.*, 2005; Yang and Van Ooij, 2004; Zhu and Van Ooij, 2003).

The use of silanes has been proposed as a protection method against corrosion for different metallic substrates, providing protection even without the application of a paint layer after treatment with a silane film (Palanivel, 2003; Zhu, 2005; Van Ooij *et al.*, 2005; Child and Van Ooij, 1999).

The objective of the present study was to evaluate the experimental parameters associated with the formation of a vinyltrimethoxysilane (VTMOS) silane film on carbon steel by the application of electrochemical techniques by evaluating its anticorrosion properties.

2. Experimental

2.1 Silane and steel used

The silane "VTMOS" was used in this study. This compound is a monosilane; that is, it has only one silicon atom, three hydrolysable groups, and one organofunctional vinyl group. In addition, this compound acts as a cross-linking agent, being a good matrix former. The steel used was a 1010 carbon steel.

2.2 Process layer formation

The VTMOS layer was formed on substrates of 1010 carbon steel with dimensions of 25 mm × 50 mm × 0.9 mm. The test

The current issue and full text archive of this journal is available at **www.emeraldinsight.com/0003-5599.htm**

Anti-Corrosion Methods and Materials
60/5 (2013) 251–258
 [ISSN 0003-5599]
[DOI 10.1108/ACMM-09-2012-1212]

The authors thank FAPESB and CAPES for financial support.

specimens were ground with 320, 400 and 600 grit emery papers, pickled in a solution of deionized water (DI) and concentrated HCl (7% v/v) for 5 min and degreased in a solution of DI and concentrated Saloclean 619 (5% v/v), in which the samples remained until silanization. This substrate treatment also was applied to steel samples that were not coated with the silane.

Solutions of the VTMOS and solvent (with different ratios of DI water/ethanol) were hydrolyzed under stirring. The silanization then was carried out by dip coating using manual immersion with controlled velocity in the previously hydrolyzed solution. The dip coated specimens were submitted to curing in an oven at different temperatures.

2.3 Planning of experiments designed to study

In order to evaluate the effect of nine quantitative factors or variables, using a reduced number of experiments, three 2^3 factorial designs were selected to carry out the study. Tables I-III show all of the prepared test specimens, based on a combination of each level of the respective factors studied in each factorial design. As there were 2^3 factorial designs, eight test specimens were required for each design. Thus, there were 24 test specimens, and one without coating as the control reference.

For Design 1, three hydrolysis factors were studied, as hydrolysis is an important stage that generally is particular or specific to each silane. In Design 2, one factor corresponding to the surface treatment of carbon steel, one to the hydrolysis, and one to the cure, were studied to verify the interaction of variables for each stage of the film formation. In Design 3, two factors of the silanization process and one of the cure were investigated; these being the factors that directly influence the formation thickness and reticulation of the film. The variables were selected based on knowledge from literature of the main variables that can influence the formation of a good film. The levels were based on a bibliographic review of values currently and most commonly applied in the silanization process.

2.4 Electrochemical techniques employed

All of the experiments were conducted in static (non-stirred) media at ambient temperature in a three-electrode cell for flat samples. The electrochemical cell used comprised an Ag/AgCl/KCl reference electrode, a platinum foil as counter electrode, and coated or uncoated steel samples as the working electrode, with an exposed area of 1 cm^2 in a 0.1 mol L^{-1} NaCl solution as the electrolyte. An EG&G/PAR potentiostat-galvanostat (model 273A), coupled to a Solartron frequency analyzer (model 1255B), was used to undertake the electrochemical tests.

First, the open-circuit potential (*E*oc vs time) was measured as a function of time. The immersion and stabilization time of the *E*oc was 1 h. For this monitoring, the Powersuite software was used.

Electrochemical impedance spectroscopy (EIS) was performed after the *E*oc monitoring. The impedance diagrams were obtained over the frequency range of 50 kHz-5 mHz, with ten readings being carried out per logarithmic decade, and with potential perturbation of 10 mV rms against *E*oc. ZPlot2 software was used for acquiring data and ZView2 for data treatment.

The real impedance value at a frequency of 0.04 Hz was considered as a quantitative response in the EIS tests, as this represents the resistance of the silane film to corrosion and the metal/medium interaction.

On completion of the *E*oc monitoring and EIS measurements, anodic and cathodic potentiodynamic polarization curves were obtained. The potential range −0.3 to 0.3 V, in relation to the *E*oc and a scan rate of 0.5 mV s^{-1} were used.

2.5 Optimized specimen

A new test specimen was prepared, based on the best results obtained for the three DOEs, and this was evaluated using the same techniques.

3. Results

3.1 Open-circuit potential

Figure 1 shows *E*oc monitoring as a function of time for the test specimens of Design 1. It can be observed that at the end of the test, that is, after 1 h immersion time, test specimen P1N6 (DI/ethanol ratio of 2:1, concentration of silane 6 percent and hydrolysis time of 2 h) showed the highest potential, indicating

Table I Matrix of experiments and specimens codes developed for the first factorial design

Variables	P1N1	P1N2	P1N3	P1N4	P1N5	P1N6	P1N7	P1N8
Ratio of DI water/ethanol	1:2	2:1	1:2	2:1	1:2	2:1	1:2	2:1
Concentration of silane (%)	6	6	2	2	6	6	2	2
Hydrolysis time (h)	48	48	48	48	2	2	2	2

Table II Matrix of experiments and specimens codes developed for the second factorial design

Variables	P2N1	P2N2	P2N3	P2N4	P2N5	P2N6	P2N7	P2N8
Grit of emery paper	2500	400	2500	400	2500	400	2500	400
Hydrolysis temperature (°C)	90	90	30	30	90	90	30	30
Cure temperature (°C)	200	200	200	200	100	100	100	100

Table III Matrix of experiments and specimens codes developed for the third factorial design

Variables	P3N1	P3N2	P3N3	P3N4	P3N5	P3N6	P3N7	P3N8
Immersion time (min)	30	2	30	2	30	2	30	2
Immersion velocity (mm $s^{-1)}$	1.6	1.6	25	25	1.6	1.6	25	25
Cure time (min)	60	60	60	60	20	20	20	20

Figure 1 Open-circuit potential (*E*oc vs time) for carbon steel in 0.1 mol L^{-1} NaCl for the first factorial design

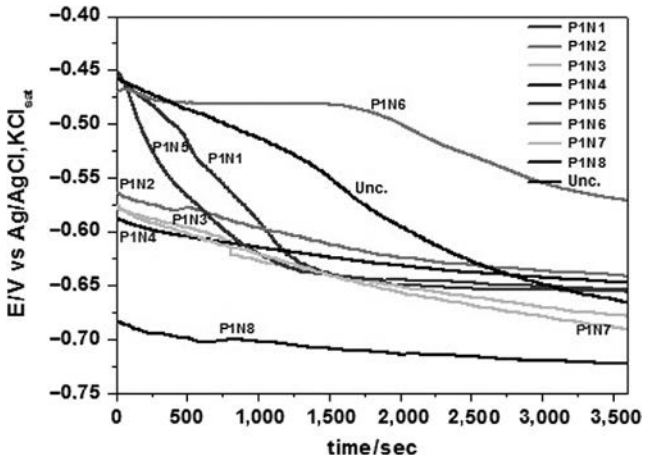

a more noble character in comparison with the other test specimens. Some test specimens even had a lower potential than the uncoated carbon steel, such as P1N3, P1N7 and P1N8, indicating a less noble nature. After 1 h of *E*oc monitoring, a quite stationary state was achieved for all the silane coated specimens.

Figures 2 and 3 show the *E*oc monitoring as a function of time for the test specimens of Designs 2 and 3, respectively. For Design 2, test specimen P2N7 (grit of emery paper of 2500, hydrolysis temperature of 30°C and cure temperature of 100°C) showed the highest *E*oc potential. For Design 3, it was observed that test specimen P3N4 (immersion time 2 min, immersion velocity 25 mm s^{-1} and cure time 60 min) and P3N3 (which differed from P3N4 only in terms of immersion time, being 30 min for this specimen), presented the highest potentials, indicating a more noble character compared with the other specimens. The uncoated specimen, in Designs 2 and 3, showed a lower potential compared with the specimens coated with a monolayer of the VTMOS, as well as a greater tendency toward a drop in the potential, revealing that the specimen is not yet at a stationary state.

Figure 2 Open-circuit potential (*E*oc vs time) for carbon steel in 0.1 mol L^{-1} NaCl for the second factorial design

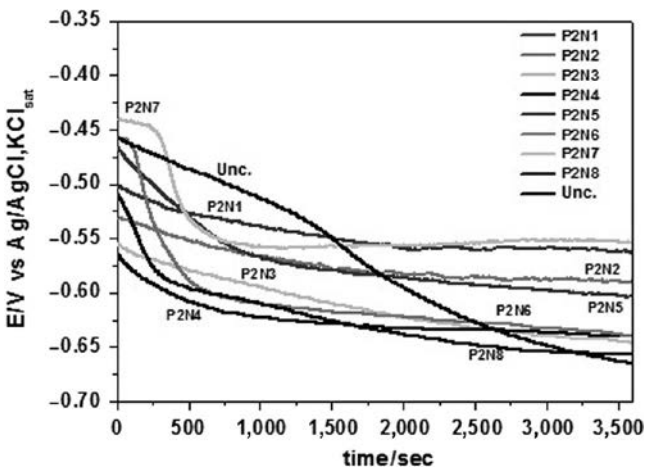

Figure 3 Open-circuit potential (*E*oc vs time) for carbon steel in 0.1 mol L^{-1} NaCl for the third factorial design

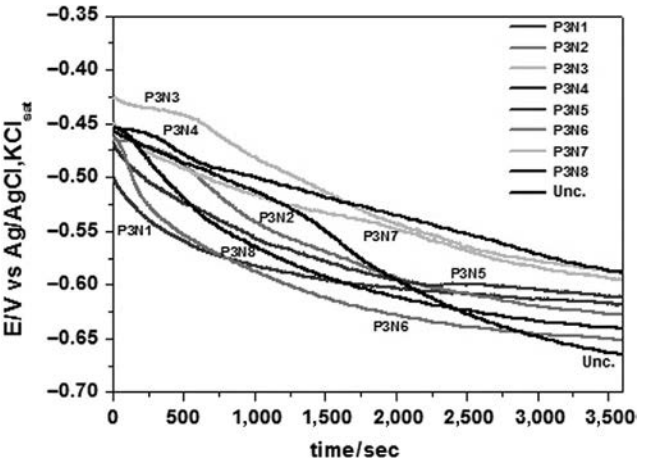

3.2 Electrochemical impedance spectroscopy

Figure 4(a) shows the Nyquist diagrams for the specimens of Design 1. It can be noted that sample. P1N1 (for which all factors were level (+), that is, the DI/ethanol ratio was 1:2, the silane concentration 6 percent and the hydrolysis time of 48 h) presented a larger capacitive arc than the other samples. Also, all of the samples coated with silane had higher real impedance than the uncoated carbon steel at 0.04 Hz frequency (represented by the point circled with the same tone as the curve). Figure 4(b) shows the Bode diagrams, where the samples coated in VTMOS present a single time constant (one maximum phase angle value) shifted to the medium and low frequency region. Only the sample P1N1 presented a high phase angle value for higher frequencies zone and a span over a wide frequency range, revealing the presence of a film and a good level of protection, evidencing a more effective response of this layer (the largest impedance modulus at lowest frequency).

Figure 5(a) shows the Nyquist diagrams for the test specimens of Design 2. It can be observed that the sample P2N7 (grit of emery paper of 2500, hydrolysis temperature of 30°C and cure temperature of 100°C) presented a much larger capacitive arc than the other samples. Furthermore, P2N3 also provided a good impedance value. However, for all other test specimens the protection index was close to that of the uncoated carbon steel, and for P2N2 and P2N8 it was lower. Figure 5(b) shows the Bode diagrams, where the samples treated with VTMOS present a single time constant, shifted to the medium and low frequency region. Only the sample P2N7 presented a high frequency zone and a span over a wide frequency range, revealing thus the presence of a protecting film imparting a better corrosion resistance to the coated specimen.

Figure 6(a) shows the Nyquist diagrams for the test specimens of Design 3. It can be observed that the sample P3N3 (immersion time of 30 min, immersion velocity of 25 mm s^{-1} and cure time of 60 min) presented a larger capacitive arc compared to other samples. All of the coated samples had higher real impedance at 0.04 Hz than the uncoated carbon steel, except sample P3N8. Figure 6(b) shows the Bode diagrams, where all of the samples treated with VTMOS present a single time constant, shifted to the medium and low frequency region. The absence of a phase angle at high frequencies may indicate the less protective nature of these films.

Figure 4 EIS diagrams in 0.1 mol L^{-1} NaCl for carbon steel coated with monolayers of VTMOS for the first factorial design and the uncoated specimen

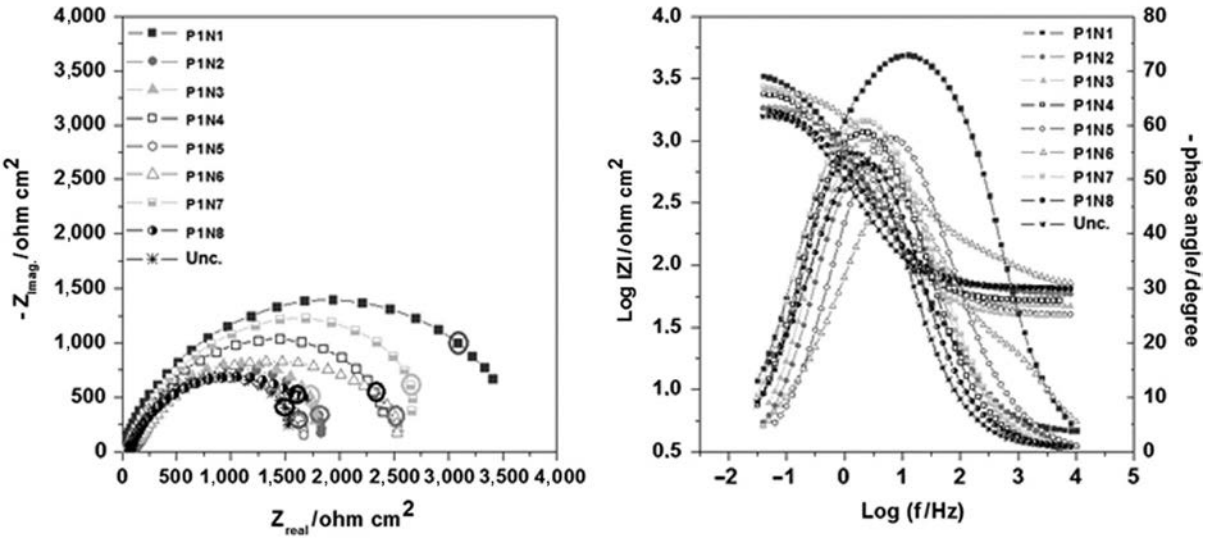

(a) (b)

Notes: (a) Nyquist diagrams; (b) Bode diagrams

Figure 5 EIS diagrams in 0.1 mol L^{-1} NaCl for carbon steel coated with monolayers of VTMOS for the second factorial design and the uncoated specimen

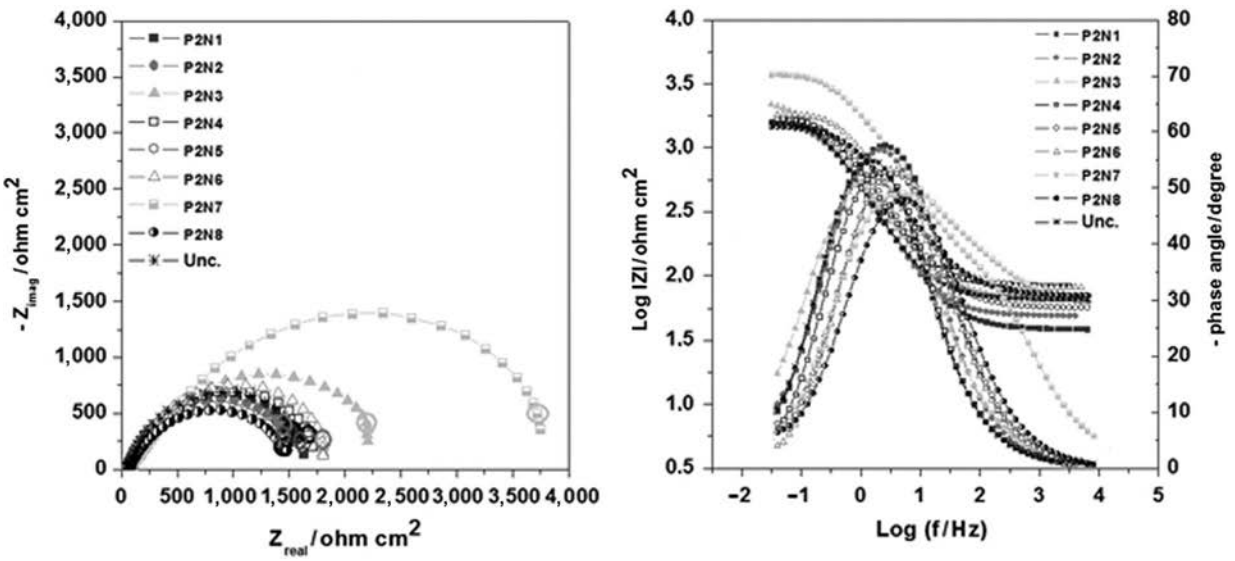

(a) (b)

Notes: (a) Nyquist diagrams; (b) Bode diagrams

Table IV shows the levels for the factors which gave the best results in the EIS test for the three factorial designs.

Figure 7 shows the Nyquist and Bode diagrams for the optimized specimen prepared based on the best EIS results obtained in the factorial design experiments, that is, respecting the levels given in Table IV. Also, it shows the specimen P2N7, which was the sample with the highest impedance value of the three factorial designs, making a direct comparison between the two. It can be observed that the real impedance at 0.04 Hz for the optimized specimen was around 20 times higher than the value obtained for P2N7, that is, 71,305 Ω cm^2 compared with 3,740.2 Ω cm^2. The Bode diagram for the optimized specimen showed two time constants, shifted to the high and low frequency region, spanning over a large frequency range, revealing the presence of a protecting film and a good level of corrosion protection. The log of impedance modulus |Z| was also higher than that of the specimen P2N7.

Equivalent circuit used to fit the experimental impedance data is shown in Figure 8. Tables V-VII show the values of the equivalent circuit elements for the fitting of EIS data, where Rs is the resistance of the electrolyte, Rf is the resistance of the film, CPE is the constant phase element representing the double

Figure 6 EIS diagrams in 0.1 mol L^{-1} NaCl for carbon steel coated with monolayers of VTMOS for the third factorial design and the uncoated specimen

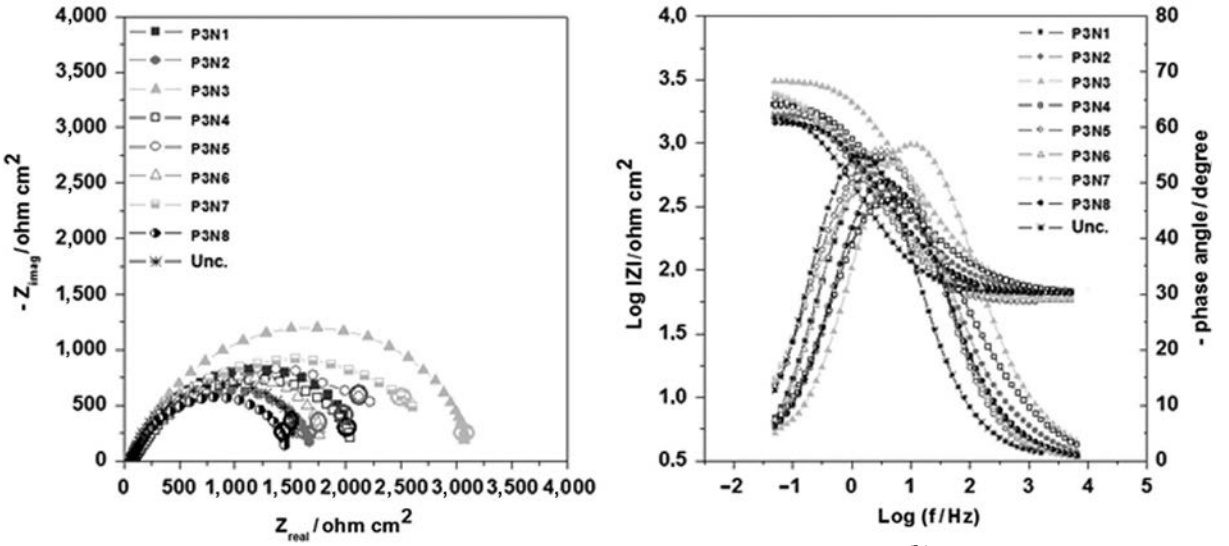

(a) (b)

Notes: (a) Nyquist diagrams; (b) Bode diagrams

Table IV Levels of factors with better results for the EIS response

Factor	Level
Ratio of DI water/ethanol	1:2
Concentration of silane	6%
Hydrolysis time	48 h
Grit of emery paper	2500
Hydrolysis temperature	30°C
Cure temperature	100°C
Immersion time	30 min
Immersion velocity	25 mm s^{-1}
Cure time	60 min

electric layer and n is the value of exponent. The calculated values of the parameters were close to experimental values. It is observed that the error values were below 3 percent, indicating a good fit. The n values were below 1, indicating a departure from the ideal behavior of a capacitor, justifying the use of CPE instead of an ideal capacitor. Table VIII shows the values of the equivalent circuit elements for the adjustments made in the optimized specimen shown in Figure 7. It is observed that Rs is negative and large error of 17 percent, which means that this equivalent circuit is not suitable for fitting the EIS data of the optimized specimen.

3.3 Anodic and cathodic potentiodynamic polarization curves

The anodic and cathodic potentiodynamic polarization curves for the three factorial designs are overlapped, as shown in Figures 9-11. The values obtained for the corrosion potential (E_{corr}) and the corrosion current density (i_{corr}) were close (the latter being in the order of 10^{-6} A cm^{-2}), indicating that the silane layer did not influence the cathodic reaction. In addition, according to the E_{corr} value, the uncoated carbon steel appears to be more noble than many of the specimens coated with VTMOS, that is, the presence of the silane film had little influence on the corrosion potential. The i_{corr} value for the uncoated sample was also lower than in the case of some of the specimens with a silane monolayer, indicating that the presence of silane film did not delay the steel oxidation reaction. The specimens P1N7, P2N5 and P3N7 had the lowest i_{corr} values, that is, they showed the best corrosion protection for their respective factorial designs. The specimens P1N6, P2N3 and P3N4 had the highest E_{corr} values. It was noted that the specimens which provided the best results in the polarization curves were not those which gave the best impedance results, however, the discrepancy between these results was not large.

4. Discussion

The results obtained in the EIS tests showed that the coating of the 1010 carbon steel with the VTMOS provides some protection, due to higher capacitive arc to the real impedance value at 0.04 Hz compared to uncoated sample, even when the phase angle at low frequencies. The lower impedance value than the uncoated carbon steel observed for three coated samples, can be explained by the probable appearance of defects in the film which adversely affected the tests, reducing the protection effect. The impedance results in the order of 1,000-4,000 Ω cm^2 can be attributed to the fact that the VTMOS binds weakly to iron and is thus easily removed by water and other solvents (Van Ooij *et al.*, 2000).

Moreover, the high impedance value of the optimized specimen shows that the film exhibits less porosity and more homogeneous, possibly forming covalent linkages of silane with the metal substrate type MeOSi, and linkages of silane with the silane neighbor type SiOSi, according to the reactions (1) and (2) (Child and Van Ooij, 1999; Xueming *et al.*, 2007):

$$SiOH_{(solution)} + MeOH_{(metal\ \ surface)} \leftrightarrow MeOSi_{(interface)} + H_2O \quad (1)$$

$$SiOH + SiOH \rightarrow SiOSi_{(silane\ \ film)} + H_2O \quad (2)$$

Figure 7 EIS diagrams in 0.1 mol L^{-1} NaCl of the sample prepared at the optimized conditions and specimen P2N7

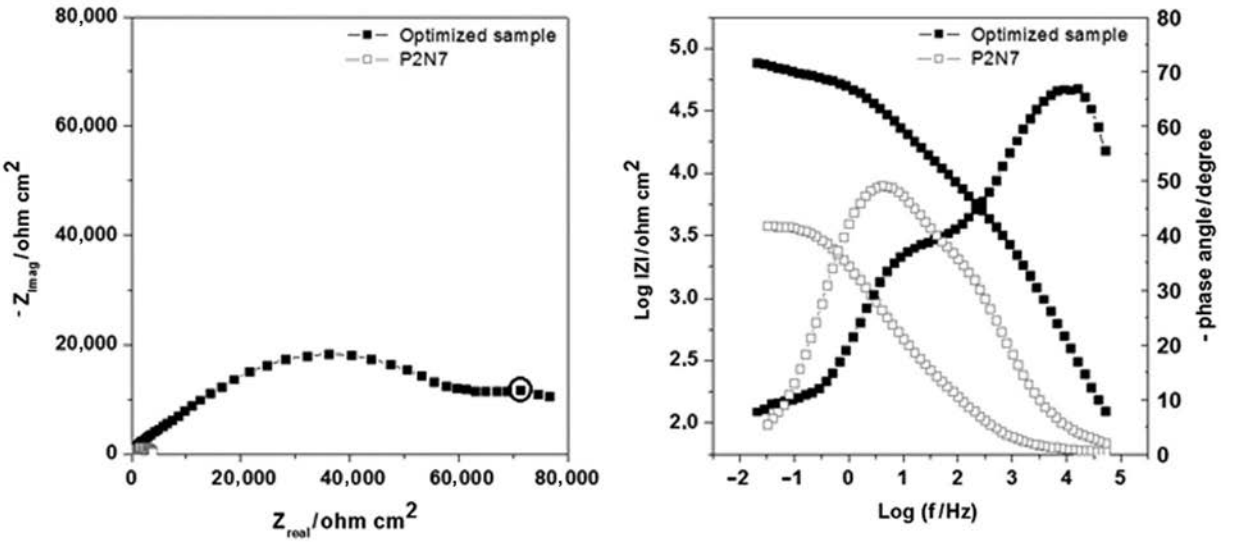

(a) (b)

Notes: (a) Nyquist diagrams; (b) Bode diagrams

Figure 8 Equivalent circuit used to fit the experimental impedance data

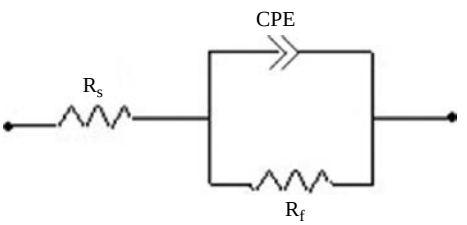

Table V Numerical results for the equivalent circuit parameters obtained from the fitting of the EIS data for the first factorial design shown in Figure 4 with the equivalent circuit in Figure 8

Specimen	Rs ($\Omega \cdot cm^2$)	% error	CPE ($\mu F \cdot cm^{-2}$)	% error	*n*	% error	Rf ($\Omega \cdot cm^2$)	% error
P1N1	4.56	0.55	240.38	0.76	0.84	0.18	3,628	0.77
P1N2	60.02	0.56	255.81	1.47	0.77	0.50	2,080	1.31
P1N3	47.53	0.33	281.85	0.83	0.81	0.28	1,801	0.85
P1N4	52.73	0.26	302.45	0.59	0.81	0.21	2,686	0.61
P1N5	40.71	0.44	173.46	1.17	0.80	0.33	1,788	0.79
P1N6	71.02	1.50	148.10	3.30	0.63	1.06	2,981	2.64
P1N7	40.13	0.34	313.85	0.69	0.80	0.24	3,262	0.90
P1N8	65.59	0.23	356.47	0.61	0.79	0.23	1,934	0.62
Uncoated	66.00	0.29	435.58	0.78	0.82	0.31	1,769	0.86

As for the equivalent circuit used, the nonideal behavior of the capacitive element that represents the silane film was also observed by other authors (Franquet *et al.*, 2003; Shaftinghen *et al.*, 2004). The setting is not suitable for optimized specimen can be explained by the presence of two time constants in the Bode diagram of the sample.

As the polarization curves, it is possible that the negative results regarding the film protection occurred due to the order in which the tests were carried out, since the polarization curves were carried out last, that is, the silane film may have deteriorated during the period in which it remained in contact with the 0.1 mol L^{-1} NaCl solution. If this was not the case then the polarization curves indicate that the VTMOS films did not effectively protect against corrosion.

5. Conclusions

Based on the results obtained in this study it can be concluded that a monolayer of the silane vinyltrimethoxysilane on 1010 carbon steel provided better properties of protection

Table VI Numerical results for the equivalent circuit parameters obtained from the fitting of the EIS data for the second factorial design shown in Figure 5 with the equivalent circuit of Figure 8

Specimen	Rs ($\Omega \cdot cm^2$)	% error	CPE ($\mu F \cdot cm^{-2}$)	% error	*n*	% error	Rf ($\Omega \cdot cm^2$)	% error
P2N1	38.92	0.18	411.58	0.43	0.81	0.15	1,784	0.47
P2N2	49.29	0.12	413.76	0.31	0.82	0.11	1,647	0.31
P2N3	65.36	0.22	449.47	0.50	0.74	0.21	2,521	0.60
P2N4	83.74	0.20	310.88	0.59	0.83	0.22	1,799	0.52
P2N5	56.98	0.25	271.33	0.74	0.80	0.24	1,595	0.59
P2N6	81.61	0.34	189.07	1.05	0.82	0.34	1,911	0.73
P2N7	59.23	1.13	140.81	2.17	0.64	0.69	4,920	2.53
P2N8	70.56	0.16	209.04	0.51	0.76	0.16	1,508	0.32
Uncoated	66.00	0.29	435.58	0.78	0.82	0.31	1,769	0.86

Table VII Numerical results for the equivalent circuit parameters obtained from the fitting of the EIS data for the third factorial design shown in Figure 6 with the equivalent circuit of Figure 8

Specimen	Rs ($\Omega \cdot cm^2$)	% error	CPE ($\mu F \cdot cm^{-2}$)	% error	*n*	% error	Rf ($\Omega \cdot cm^2$)	% error
P3N1	64.85	0.20	228.70	0.53	0.79	0.18	2,219	0.45
P3N2	69.45	0.38	202.36	1.13	0.75	0.36	1,809	0.78
P3N3	68.20	0.45	71.33	1.18	0.79	0.31	3,242	0.69
P3N4	68.30	0.62	200.57	1.60	0.69	0.53	2,337	1.30
P3N5	55.30	0.24	305.49	0.59	0.79	0.21	2,399	0.63
P3N6	57.98	0.25	243.86	0.67	0.82	0.22	1,939	0.56
P3N7	60.27	0.39	261.37	0.95	0.77	0.33	2,690	0.91
P3N8	66.76	0.34	236.60	1.03	0.78	0.33	1,554	0.72
Uncoated	66.00	0.29	435.58	0.78	0.82	0.31	1,769	0.86

Table VIII Numerical results for the equivalent circuit parameters obtained from the fitting of the EIS data for the optimized conditions specimen shown in Figure 7 with the equivalent circuit of Figure 8

Specimen	Rs ($\Omega \cdot cm^2$)	% error	CPE ($\mu F \cdot cm^{-2}$)	% error	*n*	% error	Rf ($\Omega \cdot cm^2$)	% error
Otimized	− 85.08	18.71	2.64	7.19	0.59	1.52	67,508	3.70

Figure 9 Potentiodynamic polarization curves for carbon steel coated with and without the monolayer VTMOS referring to the first factorial design in 0.1 mol L^{-1} NaCl

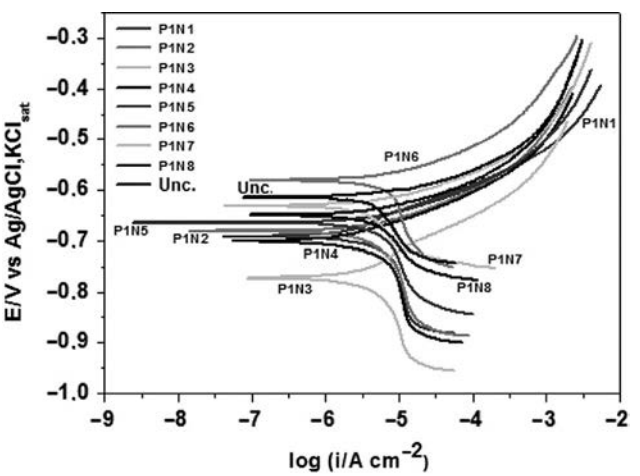

Figure 10 Potentiodynamic polarization curves for carbon steel coated with and without the monolayer VTMOS referring to the second factorial design in 0.1 mol L^{-1} NaCl

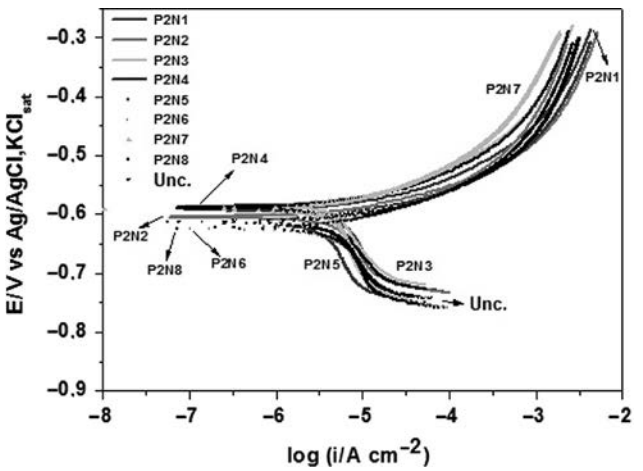

Figure 11 Potentiodynamic polarization curves for carbon steel coated with and without the monolayer VTMOS referring to the third factorial design in 0.1 mol L^{-1} NaCl

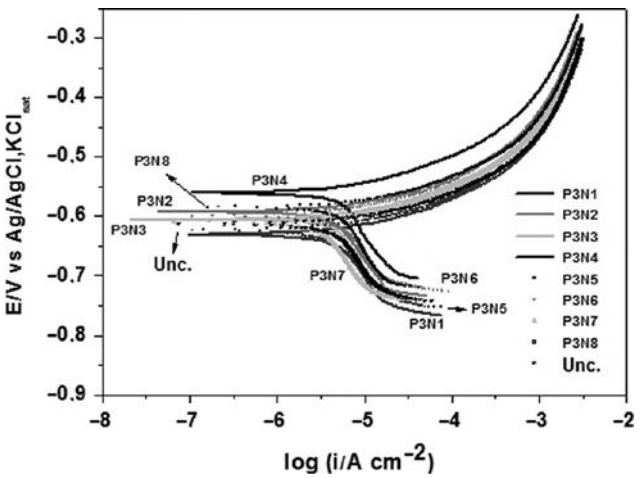

against corrosion. Thus, it could be used as a pretreatment, since it represents a promising alternative for the gradual replacement of treatments such as phosphating and chromating, representing an excellent approach considering its suitability from the environmental point of view. This conclusion is based on the values for the open-circuit potential and EIS, which were satisfactory when compared with the uncoated carbon steel.

The factorial design experiments were useful in the investigation of the optimized conditions for obtaining a silane monolayer. The optimized specimen, in terms of the EIS results, showed a considerable improvement in the corrosion resistance, being around 20 times greater compared with the best results obtained for the three factorial designs indicating the usefulness of the factorial design for planning of experiments.

References

Child, T.F. and Van Ooij, W.J. (1999), "Application of silane technology to prevent corrosion of metals improve paint adhesion", *Coatings World*, pp. 42-53.

Franquet, A., Pen, C.L., Terryn, H. and Vereecken, J. (2003), "Effect of bath concentration and curing time on the structure of nonfunctional thin organosilane layers on aluminium", *Electrochimica Acta*, Vol. 48 No. 9, pp. 1245-1255.

Metroke, T., Wang, Y.M., Van Ooij, W.J. and Schaefer, D.W. (2009), "Chemistry of mixtures of bis-[trimethoxysilylpropyl]amine and vinyltriacetoxysilane: an NMR analysis", *Journal of Sol-Gel Science and Technology*, Vol. 51 No. 1, pp. 23-31.

Palanivel, V. (2003), "Modified silane thin films as alternative to chromates for corrosion protection of aa2024-t3 alloy", dissertation, Department of Materials Science and Engineering, University of Cincinnati, Cincinnati, OH.

Palanivel, V., Huang, Y. and Van Ooij, W.J. (2005), "Effects of addition of corrosion inhibitors to silane films on the performance of AA2024-T3 in a 0.5 M NaCl solution", *Progress in Organic Coatings*, Vol. 53 No. 2, pp. 153-168.

Ran, C., Lu, W., Song, G., Ran, C. and Zhao, S. (2011), "Study on prolonging the working time of silane solution during the silylation process on carbon steel", *Anti-Corrosion Method and Materials*, Vol. 58 No. 6, pp. 328-330.

Shaftinghen, T., Pen, C.L., Terryn, H. and Horzenberger, F. (2004), "Investigation of the barrier properties of silanes on cold rolled steel", *Electrochimica Acta*, Vol. 49, pp. 2997-3004.

Van Ooij, W.J., Zhu, D., Prasad, G., Jayaseelan, S., Fu, Y. and Teresesai, N. (2000), "Silane based chromate replacements for corrosion control, paint adhesion, and rubber bonding", *Surface Engineering*, Vol. 16 No. 5, pp. 386-396.

Van Ooij, W.J., Zhu, D., Stacy, M., Seth, A., Mugada, T., Gandhi, J. and Puomi, P. (2005), "Corrosion protection properties of organofunctional silanes – an overview", *Tsinghua Science and Technology*, Vol. 10 No. 6, pp. 639-664.

Xueming, W., Guoli, L., Aiju, L. and Zuoguang, Z. (2007), "Influence of thermal curing on the fabrication and properties of thin organosilane films coated on low carbon steel substrates", *Journal of Materials Processing Technology*, Vol. 186, pp. 259-264.

Yang, H. and Van Ooij, W.J. (2004), "Plasma-treated triazole as a novel organic slow-release paint pigment for corrosion control of AA2024-T3", *Progress in Organic Coatings*, Vol. 50 No. 3, pp. 149-161.

Zhu, D. (2005), "Corrosion protection of metals by silane surface treatments", PhD thesis, Department of Materials Science and Engineering of the College of Engineering, University of Cincinnati, Cincinnati, OH.

Zhu, D. and Van Ooij, W.J. (2003), "Corrosion protection of AA 2024-T3 by bis-[3-(triethoxysilyl)propyl]tetrasulfide in neutral sodium chloride solution, part 1: corrosion of AA 2024-T3", *Corrosion Science*, Vol. 45 No. 10, pp. 2163-2175.

Corresponding author

Bruno Souza Fernandes can be contacted at: brunofernandes 4321@gmail.com